Provided for non-commercial research and education use.
Not for reproduction, distribution or commercial use.

Volume 254, No. 3, 30 November 2007 ISSN 0169-4332

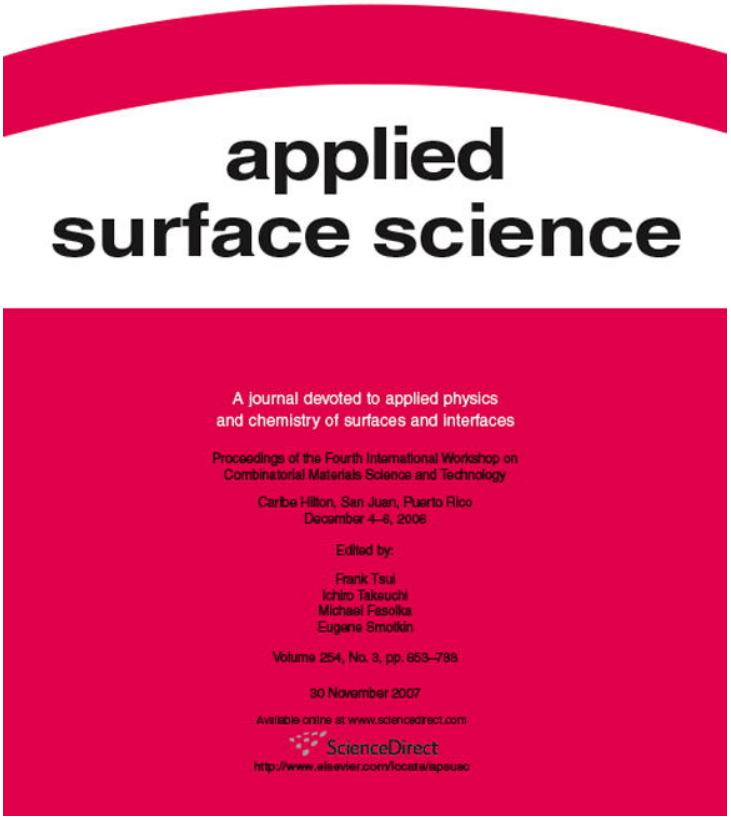

This article was published in an Elsevier journal. The attached copy is furnished to the author for non-commercial research and education use, including for instruction at the author's institution, sharing with colleagues and providing to institution administration.

Other uses, including reproduction and distribution, or selling or licensing copies, or posting to personal, institutional or third party websites are prohibited.

In most cases authors are permitted to post their version of the article (e.g. in Word or Tex form) to their personal website or institutional repository. Authors requiring further information regarding Elsevier's archiving and manuscript policies are encouraged to visit:

http://www.elsevier.com/copyright

Author's personal copy

Available online at www.sciencedirect.com
ScienceDirect
Applied Surface Science 254 (2007) 714–719
applied surface science
www.elsevier.com/locate/apsusc

High-resolution X-ray diffraction studies of combinatorial epitaxial Ge (0 0 1) thin-films on Ge (0 0 1) substrates

Yuncheng Zhong [a], Yong S. Chu [a,*], Brian A. Collins [b], Frank Tsui [b]

[a] *Advanced Photon Source, Argonne National Laboratory, Argonne, IL 60439, United States*
[b] *Department of Physics and Astronomy, University of North Carolina, Chapel Hill, NC 27599, United States*

Received 6 February 2007; accepted 10 May 2007
Available online 13 July 2007

Abstract

We report high-resolution X-ray diffraction studies of combinatorial epitaxial Ge (0 0 1) thin-films with varying doping concentrations of Co and Mn grown on Ge (0 0 1) substrates. The crystalline structure of the epitaxial thin-film has been determined using crystal-truncation rod (CTR) measurements and fitting analysis. By analyzing the fine interference fringes in the CTR intensity profile, strain sensitivity of ~0.003% has been achieved. Using this method, the evolution of interfacial structures has been quantified as a function of doping concentration.
© 2007 Elsevier B.V. All rights reserved.

PACS : 61.10.Nz; 68.55.−a; 61.80.−x

Keywords: X-ray diffraction; Crystal-truncation rods; Combinatorial thin-film; Strain

1. Introduction

Controlling electronic and magnetic properties of semiconductors by doping them with magnetic impurities is an important objective for the science and technology of spintronics. One of the primary scientific challenges is the ability to retain high levels of magnetic impurities while maintaining stable epitaxial growth without dopant-induced phase separation. Transition metals have been used successfully to dope Ge during epitaxial growth, producing high quality epitaxial films that exhibit promising electronic and magnetic behavior [1–7]. Using combinatorial synthesis and high-resolution X-ray diffraction measurements, we have demonstrated that complementary doping with Co and Mn can reduce the interfacial strain between the Ge (0 0 1) film and the Ge (0 0 1) substrate, thus maintaining interfacial coherence at doping concentrations up to 14 at.% [6,7]. High-resolution X-ray strain measurements on combinatorial epitaxial thin-films are, however, non-trivial and require the experimental considerations and analysis methods specific to this class of materials.

Typical combinatorial samples have a composition gradient along either one-direction with respect to the growth plane (‘‘binary’’ composition-spread) or two-directions (‘‘ternary’’ composition-spread). Consequently, the sampling area or footprint of a strain measurement must be sufficiently small in order to insure minimal composition variation [8]. This requirement rules out the application of grazing-incident X-ray diffraction, in which the use of the evanescent wave makes it possible to measure the in-plane strain of the film while completely avoiding the strong background signal from the substrate [9]. In the Ge (0 0 1) on Ge (0 0 1) epitaxial system that we investigate, determining the strain of the film is rather difficult, owing primarily to the following reasons. First, the film reflections are all completely ‘‘buried’’ under those of the substrate, owing to the identical crystalline structures and the low level of strain (<0.1%) between the two. In other words, the film reflections are extremely close to those of the substrate, while their intensities are many orders of magnitude lower than the substrate’s. Second, the diffraction pattern of the thin film does not consist of a single set of reflections but rather a seemingly complicated interference pattern. The interference pattern arises from the coherent quality of our epitaxial thin-films produced by the advanced combinatorial MBE synthesis,

* Corresponding author at: Argonne National Laboratory, 9700 S. Cass Ave., Argonne, IL 60439-4856, United States. Tel.: +1 630 252 0150; fax: +1 630 252 9303.
E-mail address: ychu@aps.anl.gov (Y.S. Chu).

0169-4332/$ – see front matter © 2007 Elsevier B.V. All rights reserved.
doi:10.1016/j.apsusc.2007.05.088

Author's personal copy

such that the scattering amplitude from each of the atomic layers in the film interferes *coherently* with that from the counterparts in the substrate. The presence of the atomically smooth interfaces thus gives rise to well-defined crystal-truncation rod (CTR) intensity [10,11]. In this paper we present our method for measuring the CTR profile and analyzing their intensities in order to quantify the interfacial strain and other structural parameters of the combinatorial epitaxial thin-films.

2. Experimental

2.1. Samples

Synthesis of Co and Mn doped Ge (0 0 1) films was carried out using an advanced combinatorial MBE system [12]. Control of the linear composition gradient was accomplished by a combination of precision masks and sample manipulation, and real-time flux control using atomic absorption spectroscopy. Electron beam hearths were used for evaporating Ge and Co and an effusion cell was used for Mn at a based pressure of 10^{-11} Torr. The Ge (0 0 1) substrates were treated *in situ* through annealing–deposition cycles in order to produce atomically smooth surfaces for the study. The combinatorial MBE growth was carried out at a growth temperature of 250 °C and flux of ~0.1 Å/s. Real-time scanning reflection high-energy electron diffraction (RHEED) imaging was used to monitor the structural evolution across the sample during synthesis. Complementary experiments using *in situ* scanning probe microscopy (SPM) and cross-sectional high-resolution transmission electron microscopy (HRTEM) were also carried out to characterize the film quality before the X-ray investigation. A typical sample is ~10 mm long with a doping concentration gradient of ~2 atomic percent (at.%) per mm.

2.2. X-ray diffraction measurement

Structural investigation of the combinatorial epitaxial thin-films was carried out at the beamline 2-BM of the Advanced Photon Source (APS) in Argonne National Laboratory. An X-ray mirror with Cr coating was used to suppress the X-ray energy above 20 keV, and a double-bounce Si (1 1 1) crystal monochromator was used to select monochromatic X-rays with 10.5 keV in energy. A focused X-ray beam was produced using bendable Kirkpatrick-Baez (KB) X-ray mirrors. The X-rays are focused first vertically using a 100-mm long vertical mirror and then horizontally using a 200-mm long horizontal mirror. Unlike most of the KB mirrors for synchrotron use, this KB system was designed with a long nominal working distance of 400 mm from the end of the second mirror to the center of the 4-circle diffractometer. This setup provided sufficient range of motion within the diffractometer for the X-ray diffraction investigation. We used a beam size of 5 μm × 5 μm with the focused X-ray flux of 10^9 photons/s. Considering typical incident angles of 15–30° onto a sample during the XRD measurement with composition gradient of 2 at.% per mm, the composition resolution due to the finite beam size is 0.02–0.04%. X-ray fluorescence intensities from Co and Mn were measured using an energy-dispersive Si-drift diode detector [13]. The doping concentrations were determined by comparing the fluorescence intensities from the sample and those from reference samples with known amounts of Co and Mn. The resulting experimental uncertainty for determining the absolute concentration is ~25%, including both statistical and systematical errors.

Since our epitaxial films are significantly thicker (~1000 Å) than a typical sample for the CTR measurements, we adopted a slightly different measurement method from the conventional approach [11]. The large film thickness produces fast-varying oscillatory fringes, so sampling over a narrow range in the reciprocal space (~0.1 in L) would be sufficient to obtain large number of the interference fringes needed to determine the strain of the film accurately. Second, the usual background subtraction of the CTR intensity using a ''transverse'' scan with respect to the L-direction (i.e. θ-scan at a fixed L) is difficult to perform at the L positions close to the Bragg peak owing to its high intensity, and thus only line scans along the [0 0 1] growth direction (i.e. L-direction) through (1 1 3) and (0 0 4) reflections of the substrate were performed without the usual background subtraction. The diffuse scattering intensity that originates from the Bragg peak is instead included in our fitting analysis, as discussed in Section 3 below. Furthermore, our measurements show that within the range of L, the background intensity is negligible (about a factor of several to 10 times lower than the CTR intensity), and that the transverse width of the CTR intensity is nearly constant except for L very near the Bragg peak [14]. Therefore, the CTR intensities obtained using the line scans do not present any technical problems when they are fitted by the model.

3. Results and discussion

We carried out high-resolution reciprocal-space mapping in planes defined by the vectors [0 0 L] and [H H 0] and centered on several Bragg reflections. Typically, epitaxial thin-films under the influence of epitaxial constraints exhibit different strains along directions perpendicular and parallel to the interface that are described by elastic theory [15]. For a Ge (0 0 1) thin-film grown on Ge (0 0 1) substrate, the strains along two in-plane directions, <1 0 0> and <0 1 0>, are identical due to the biaxial symmetry, and thus the strain state of the film requires measurement of its lattice parameters only in the directions normal and parallel to the interface. Previous studies using *in situ* scanning reflection high-energy electron diffraction (RHEED) during the growth and *ex situ* cross-sectional high-resolution transmission electron microscopy (HRTEM) measurements indicate that the doped Ge (0 0 1) thin-films are coherent at the interface [6–7]. The high-resolution X-ray diffraction study also shows that the in-plane lattice parameters of the film match those of the substrate within an instrumental resolution of about 10^{-4}.

While these measurements suggest that the Ge (0 0 1) thin-film is most likely to be lattice-matched to the substrate parallel to the surface, we offer additional evidence. Fig. 1 shows the 0 0 L (solid line) and 1 1 L (open circles) CTR profiles

Author's personal copy

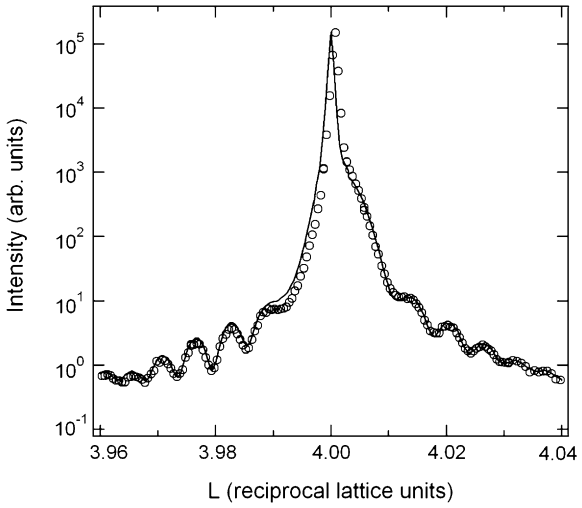

Fig. 1. The 0 0 L (solid line) and 1 1 L (circles) CTR profiles measured at doping concentration of 2.3 at.% Co. The 1 1 L CTR intensity profile has been shifted in L by 1.001, as discussed in the text.

measured at Co doping concentration of 2.3 at.%. For the 0 0 L CTR profile, the sharp intensity at $L = 4$ corresponds to (0 0 4) Bragg reflection of the substrate, while the intensity fringes correspond to the diffraction pattern of the thin-film. As discussed below, the asymmetric intensity shoulder around the (0 0 4) Bragg peak is due to a small (0.1%) compressive surface-normal strain of the film. Since the 0 0 L CTR is insensitive to the lateral atomic position of the film, this CTR intensity profile contains the contribution from all of the atomic layers in the film, regardless of the in-plan strain, so long as these layers can scatter coherently with the substrate and one another. In contrast, only the commensurate (i.e. in-plane lattice matched) atomic layers of the film contribute to the 1 1 L CTR profile. In Fig. 1, the 1 1 L CTR profile measured at the same composition is shifted by 1.001 and superimposed to that of the 0 0 L. The shift is to account for the difference in the L position between (1 1 3) and (0 0 4) reflections and the 0.1% compressive strain in the film. Without any intensity adjustment, the two data sets are strikingly identical, except for L values immediately around the Bragg peak, where the intensity difference is caused by the afore mentioned shift in favor of aligning the diffraction pattern of the film rather than the substrate counterpart. If the film lattice were to be relaxed, a noticeable intensity drop and phase shift would occur in the 1 1 L CTR intensity profile with respect to that of the 0 0 L, and therefore, the matching interference fringes between the two profiles provide a strong evidence for all of the atomic layers in the film to be in-plane lattice-matched with the substrate.

Detailed structural properties of the films, including the strain normal to the surface, have been quantified by fitting the measured CTR intensity profiles to the form $I(L) = s|F(L)|^2 + B(L)$. Here, the reciprocal lattice unit L is defined as $qa_s/2\pi$ in terms of the momentum transfer wave vector q and the substrate lattice parameter a_s; the intensity $I(L)$ consists of two contributions, one from the structure factor for the unit cell, $F(L)$, with an overall scale factor s, and another from the background intensity, $B(L)$. A Voigt function at a constant L of 3 with five fitting parameters, including peak height, Gaussian width, Lorentzian width, Voigt shape, and a constant background, is used to describe the latter. The former can be expressed as [10],

$$F(L) = e^{-\frac{q^2\sigma_s^2}{2}} \frac{1}{1 - \exp(-i2\pi L)} + e^{\frac{-q^2\sigma_f^2}{2}} \sum_{n=0}^{N} \exp\left(i2\pi L \frac{a_\perp}{a_s}\right) \quad (1)$$

In the first term of Eq. (1), $[1 - \exp(-i2\pi L)]^{-1}$ is the structure factor of the substrate (see discussions below for Fig. 3a), and in the second term $\sum_{n=0}^{N-1} \exp(i2\pi L a_\perp/a_s)$ corresponds to the contribution from the film with N number of unit cells and a constant surface-normal lattice parameter $a_\perp$ · a_s has been held at the bulk Ge value of 5.65795 Å. The second term is equivalent to the "N-slit interference function" that gives rise to the interference fringes shown in Fig. 1 with the position of the interference fringes with respect to that of the Bragg peak controlled by the ratio $a_\perp/a_s$ [16]. The prefactors, $e^{-q^2\sigma^2/2}$, describe the Debye-Waller intensity reductions for the substrate (denoted by subscript s) and the film (denoted by subscript f) with σ the RMS displacement amplitude of atoms from their equilibrium positions. The Debye-Waller factor, B, is related to σ through $B = 8\pi^2\sigma^2$ [17]. In the fitting model, the magnitude of σ should be interpreted as the variance in the unit cell position, or the magnitude of the crystalline disorder rather than the time-averaged thermal fluctuations of the lattice. We also have made several assumptions. First, the atomic form factors of the substrate and the film are assumed to be identical and thus omitted in Eq. (1). Second, since the measured CTR profiles were collected over a narrow range of L (<0.1), effects associated with surface roughness and atomic positions within the unit cell are not significant and excluded in the modeling. Third, the strain of the film is initially assumed to be uniform throughout the entire film.

The simplified model with uniform strain is put to test in Fig. 2a, where a comparison is made between the model fit (blue curve) and the data along [1 1 L] for Co doping concentration of 1.0 at.%. Despite the simplicity, the model fit is excellent, producing the key features in the data. However, a closer inspection at $L > 3$ reveals a rather systematic deviation of the fit from the data. In order to examine the quality of the fit for the film contribution to the intensity, the CTR profiles have been normalized by dividing them by the calculated substrate CTR intensity profile [the first term in Eq. (1)], as are shown in Fig. 2b, thus enhancing the effects of the film. For $L > 3$, the simple fit (blue curve) produces incorrect intensity profile in fringe intensity and positions with respect to the measurement (circles), while for $L < 3$ the fit is almost perfect. This systematic deviation can be interpreted as an additional phase shift of the interference fringe on the right side of the Bragg peak. The surface-normal strain of the epitaxial film not being completely uniform can account for this additional phase shift. Interdiffusion of dopants, particularly at the interface, can give rise to spatial inhomogeneities in concentration leading to a corresponding non-uniform strain. On the other hand, effects of dynamical scattering in a ~1000 Å

Author's personal copy

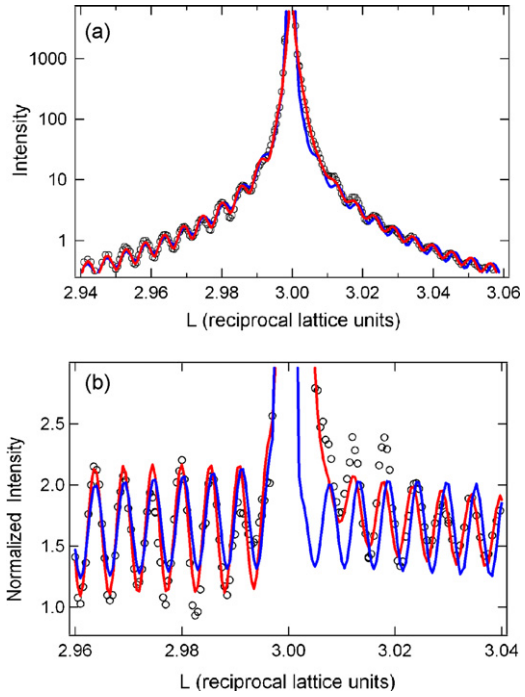

Fig. 2. Comparison between the fits and the measurements. The blue line represents the best fit using a film with uniform strain (Eq. (1)). The red line represents the best fit by adding a thin interfacial layer to the thicker film with uniform strain, as detailed in the text. (a) 1 1 L rod profile and (b) 1 1 L rod profile divided by the calculated intensity contribution from the substrate (the first term in Eq. (1)). The data were measured at doping concentration of 1.0 at.% Co (Color online).

thick film can only give rise to a negligible amount of additional phase shift. Therefore, within the kinematical approximation, the simple uniform strain model [the second term in Eq. (1)] has been modified by introducing an additional interfacial layer with N' number of unit cells and a different surface-normal lattice parameter, $a'_\perp$. This leads to $\sum_{n=0}^{N'-1} \exp\left(\mathrm{i}2\pi L a'_\perp/a_s\right) + \sum_{n=N'}^{N-1} \exp(\mathrm{i}2\pi L a_\perp/a_s)$ replacing the simple N-slit interference function $\sum_{n=0}^{N-1} \exp(\mathrm{i}2\pi L a_\perp/a_s)$. As shown in the solid lines in Fig. 2 with $N' = 9$ and $a'_\perp/a_s = 1.0001$, the addition of a thin interfacial layer between the substrate and the film does provide the necessary phase shift, and thus improves the fit significantly.

As mentioned above, the inclusion of a thin interfacial layer is consistent with finite interdiffusion of dopants. The presence of dopant-rich and poor regions, such as an interfacial dopant-poor layer owing to diffusion of dopants into the substrate, can give rise to corresponding regions with different lattice parameters, even in the absence of dislocations. The existence of these regions and their spatial extent are being examined currently using probes that are sensitive to this effect, including scanning TEM (STEM) spectroscopy and local electrode atom probe (LEAP) tomography techniques. At the meantime, in the interest of keeping the fitting model as simple as possible, we have chosen to use this two-layer model for analyzing the data, from which the "average" strain of the thin-film in terms of $a_\perp/a_s$ is determined, as presented in the remainder of this paper. Here, the ratio $a_\perp/a_s$ can be readily converted to the surface-normal strain of the film $\varepsilon_\perp \equiv a_\perp/a_s - 1$. Throughout

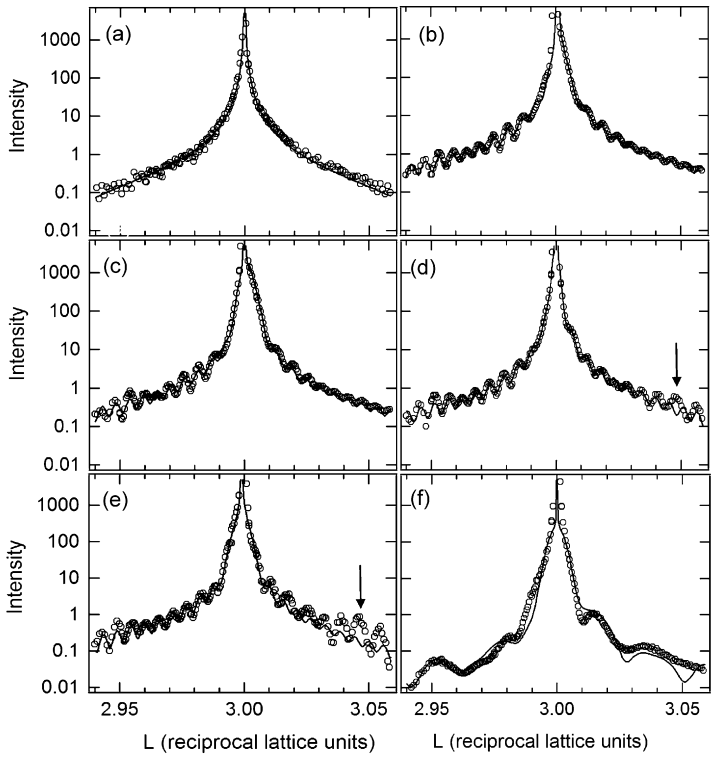

Fig. 3. The evolution of the measured CTR profiles with increasing doping concentration: (a) undoped; (b) 1.4 at.% Co; (c) 2.3 at.% Co; (d) 4.7 at.% Co and 1.2 at.% Mn; (e) 7.2 at.% Co and 3.3 at.% Mn; and (f) 8.5 at.% Co and 4.6 at.% Mn. Arrows indicate additional features that deviate from a uniformly strained crystalline structure. At a combined doping concentration of ~13 at.% (f), the coherent interference fringe pattern is lost.

Author's personal copy

Table 1
List of the structural fitting parameters of the combinatorial Ge epitaxial films

Data set	Co (at.%)	Mn (at.%)	σ_f/σ_s	N	$\varepsilon_\perp$ (%)
b	1.4	0	1.3 ± 0.3	182 ± 2	-0.105 ± 0.003
c	2.3	0	1.4 ± 0.3	179 ± 2	-0.129 ± 0.003
d	4.7	1.2	2.0 ± 0.5	178 ± 2	-0.032 ± 0.003
e	7.2	3.3	1.9 ± 0.7	177 ± 2	-0.016 ± 0.007
f	8.5	4.6	6 ± 2	47 ± 5	–

Columns from left to right are as follows. The data sets b–f correspond to those shown in Fig. 3b–f, respectively. The doping concentrations of Co and Mn are given in atomic percent. σ_f/σ_s is the ratio of the disorder magnitudes between the film and the substrate. N is the number of unit cells of the film that scatters coherently with the substrate lattice. $\varepsilon_\perp$ is the film strain normal to the surface.

the fitting analysis, we have kept $N' = 9$ and allowed the value of $d'_\perp/a_s$ to vary with an upper bound of $\sim 5 \times 10^{-5}$ from unity.

Fig. 3 shows the evolution of the measured CTR intensity profiles as a function of increasing doping concentration in the film along with the best fit (solid line) using the two-layer kinematical model with the essential fitting parameters of the film listed in Table 1. As expected, the CTR profile collected from a bare substrate shown in Fig. 3a contains no fringes but only the contribution from the substrate. In Fig. 3b–e with film thickness of 1001–1029 Å and increasing doping concentration, a systematic shift in the position of the intensity fringes around the Bragg peak at $L = 3$ is observed. Using the fitting analysis, the film is determined to be under a greater compressive strain as the Co doping concentration is increased from 1.4 at.% to 2.3 at.%, owing to the smaller atomic size of Co with respect to Ge. At doping concentration of 4.7 at.% Co and 1.2 at.% Mn, the compressive strain is, however, relieved considerably, despite the higher doping concentration of Co. At doping concentration of 7.2 at.% Co and 3.3 at.% Mn, the surface-normal strain is nearly zero. This effect can be attributed to the compensation of strain by the different atomic sizes of the co-dopants (Co and Mn) with respect to the Ge host lattice, as discussed in detail elsewhere [7]. Here we focus on the high-resolution diffraction technique for probing such effects.

With increasing doping concentration, the measured CTR profile starts to display features that cannot be produced by our simplistic model. For example, the profile for 4.7 at.% Co and 1.2 at.% Mn (Fig. 3d) contains one intensity fringe (indicated by an arrow) whose position is completely out of phase with the fit, while interestingly, all other fringes are in perfect alignment with the fit. At a combined doping concentration of 10.5 at.% (Fig. 3e), the effect becomes more pronounced. The observed behavior suggests that there may be additional frequency component with a much larger period than the fringes, which corresponds length scales much smaller than the film thickness. Though the exact structures corresponding to these features are not known, the data clearly indicate that the strain uniformity begins to deteriorate as doping concentration increases, so the observed phase shift in CTR intensity may very well be related to the diffusion-induced dopant concentration inhomogeneities mentioned above. In addition, it is also possible that the thin-film at this composition may have a higher level of dislocation density and a larger number of grain boundaries. However, both interpretations appear to be consistent with a modest increase in the magnitude of disorder in the film, parameterized by the value of σ_f/σ_s. In order to elucidate the doping concentration related structural phenomena, spatially resolved investigations using STEM spectroscopy and LEAP tomography need to be carried out as mentioned above, in combination with further CTR investigations by collecting intensities over a much larger range in reciprocal space and analyzed using more sophisticated fitting models.

Further doping beyond the critical level causes a qualitative change in the structure of the Ge epitaxial thin-film, as can be seen in Fig. 3f. The intensity of the fringes is about 10 times lower away from the Bragg peak, and the period of the fringes is significantly larger with much less regularity. At this point our simple model does not produce a good fit, and consequently, the surface-normal strain cannot be determined accurately. However, some other parameters from the fit can still provide useful and perhaps quantitative information. For example, the number of unit cells from the fit is only 47. This reduction does not mean that the film is physically thinner at this composition, but instead it corresponds to a decrease in the number of unit cells that are still scattering ''coherently'' with the substrate. In other words, if the film contains a larger number of domains separated by a network of domain boundaries, the scattering phases from the individual domains are not correlated with each other and cannot interfere coherently with that from the substrate; only coherent domains contribute to the measured CTR profile. In addition the amount of disorder, indicated by the value of σ_f/σ_s, becomes significant at this composition (Table 1).

The structural evolution described above with a loss of structural coherence above a critical doping concentration appears to be common to all epitaxial thin-films of transition metal doped Ge we have investigated thus far, regardless of the specific doping elements. The onset of this epitaxial instability coincides with that of rough 3D-like growth observed initially by *in situ* RHEED measurements [6,7]. Our ability to use X-rays to measure the structural transition as a function of composition is not only important for obtaining quantitative structural parameters with higher spatial and compositional resolution, but also essential for studying ternary combinatorial samples for which *in situ* RHEED measurements are unrealistic owing to the large footprint of the RHEED beam.

Sampling of a large number of interference fringes in the CTR profile provides a much higher sensitivity to the small change in the strain of the thin-film than measuring the position of a single peak, analogous to the use of optical interferometry to enhance precision and sensitivity. Furthermore, the strain of the thin-film is determined from the relative shift of the intensity fringes with respect to the position of the substrate Bragg peak, which is independent of the uncertainties in the absolute calibration of the diffraction angles (i.e. 2θ) and the energy of the incident X-rays. The resulting sensitivity for strain from the CTR structural analysis is determined to be about 0.003% (the uncertainties in Table 1).

Author's personal copy

4. Summary

High-resolution X-ray diffraction measurements have been performed on the combinatorial epitaxial doped Ge (0 0 1) thin-films grown on Ge (0 0 1) substrates. The strain states and structural ordering of the films have been examined and quantified as a function of the doping concentrations of Mn and Co, using CTR measurements and analysis. The details of our structural model and the fitting analysis along with their application to quantifying the strain and other structural parameters have been discussed. The method is proven to be well suited for structural studies of high quality combinatorial epitaxial thin-films, and specifically it can provide a high sensitivity for strain of $\sim$0.003%.

Acknowledgement

We thank Liang He for growing the samples. Use of the Advanced Photon Source is supported by the U. S. Department of Energy, Office of Sciences, Office of Basic Energy Sciences, under Contract No. DE-AC02-06CH11357. The work is supported in part by DOE BES DE-FG02-05ER46216 for the measurements and student support, by NSF DMR-0441218 for MBE synthesis, and by DOD W911NF-05-1-0173 for MBE instrumentation. Authors also acknowledge an APS subcontract 5F-00428 for partial student support.

References

[1] Y.D. Park, A.T. Hanbicki, S.C. Erwin, C.S. Hellberg, J.M. Sullivan, J.E. Mattson, T.F. Ambrose, A. Willison, G. Spanos, B.T. Jonker, Science 295 (2002) 651–654.
[2] S. Choi, et al. Appl. Phys. Lett. 81 (2002) 3606–3608.
[3] S. Cho, Y. Kim, S. Choi, S.C. Hong, B.J. Kim, J.H. Jung, Y.C. Kim, J.B. Ketterson, Phys. Rev. B 66 (2002) 033303.
[4] V. Ko, K.L. Teo, T. Liew, T.C. Chong, Appl. Phys. Lett. 89 (2006) 042504.
[5] R.R. Gareev, et al. Appl. Phys. Lett. 88 (2006) 222508.
[6] F. Tsui, L. He, L. Ma, A. Tkachuk, Y.S. Chu, K. Nakajima, T. Chikyow, Phys. Rev. Lett. 91 (2003) 177203.
[7] F. Tsui, L. He, A. Tkachuk, S. Vogt, Y.S. Chu, Phys. Rev. B 69 (2004) 081304R.
[8] Y.S. Chu, A. Tkachuk, S. Vogt, P. Ilinski, D.A. Walko, D.C. Mancini, E.M. Dufresne, L. He, F. Tsui, Appl. Surf. Sci. 223 (2004) 175–182.
[9] W.C. Marra, P. Eisenberger, A.Y. Cho, J. Appl. Phys. 50 (1979) 6927–6933.
[10] I.K. Robinson, D.J. Tweet, Rep. Prog. Phys. 55 (1992) 599–651.
[11] I.K. Robinson, Surface Crystallography, Handbook on Synchrotron Radiation, Vol. III, edited by D.E. Moncton & G.S. Brown. North-Holland, 1991.
[12] F. Tsui, L. He, Rev. Sci. Inst. 76 (2005) 062206.
[13] S. Vogt, Y.S. Chu, A. Tkachuk, P. Ilinski, D. Walko, F. Tsui, Appl. Surf. Sci. 223 (2004) 214–219.
[14] L. He, B.A. Collins, F. Tsui, Y. Zhong, S. Vogt, Y.S. Chu, J. Vac. Sci. Tech. B 25 (2007) 1217.
[15] I.C. Noyan, J.B. Cohen, Residual Stress, Sprinter-Verlag, New York, 1987.
[16] Q. Shen, S. Kycia, Phys. Rev. B 55 (1997) 15791–15797.
[17] L.-M. Peng, G. Ren, S.L. Dudarev, J.J. Whelan, Acta Cryst. A52 (1996) 456–470.